Available online at www.sciencedirect.com
ScienceDirect
Neuroscience Letters 420 (2007) 6–11
Neuroscience Letters
www.elsevier.com/locate/neulet

# Complex changes in ecto-nucleoside 5′-triphosphate diphosphohydrolase expression in hypoxanthine phosphoribosyl transferase deficiency

Veronika Lorenz [a], Cibele S. Pinto [b], Roland Seifert [a,b,*]

[a] *Department of Pharmacology and Toxicology, University of Regensburg, Germany*
[b] *Department of Pharmacology and Toxicology, University of Kansas, Lawrence, USA*

Received 6 March 2007; received in revised form 21 March 2007; accepted 1 April 2007

**Abstract**

Lesch-Nyhan disease is caused by a deficiency of the purine salvage enzyme, hypoxanthine phosphoribosyl transferase (HPRT). The link between HPRT deficiency and the neuropsychiatric symptoms is unknown. In rat B103 neuroblastoma cell membranes and mouse Neuro2a neuroblastoma cell membranes, nucleoside 5′-triphosphatase (NTPase) activity is substantially reduced, whereas in fibroblast membranes from HPRT knock-out mice, NTPase activity is increased. Candidate genes for these NTPase activity changes are ecto-nucleoside 5′-triphosphate diphosphohydrolases (NTPDases). Therefore, we studied expression of NTPDases in B103 cells, Neuro2a cells and skin fibroblasts by reverse transcriptase polymerase chain reaction and restriction enzyme digestion of amplified cDNA fragments. In B103 cells, expression of NTPDases 1, 3 and 6 decreased, whereas expression of NTPDases 4 and 5 increased in HPRT deficiency. In Neuro2a cells, expression of NTPDases 3–6 increased in HPRT deficiency. In fibroblasts, NTPDase 3 expression decreased, and expression of NTPDases 4–6 increased in HPRT deficiency. Collectively, there are complex decreases and increases in NTPDase isoform expression in HPRT deficiency that depend on the specific cell type and species studied. These changes in NTPDase expression may reflect an (insufficient) attempt of cells to compensate for the changes in nucleotide metabolism caused by HPRT deficiency.


*Keywords:* Lesch-Nyhan disease; Hypoxanthine phosphoribosyl transferase; Ecto-nucleoside 5′-triphosphate diphosphohydrolase; Fibroblasts; Neuroblastoma cells

Lesch-Nyhan disease (LND) is caused by a defect of hypoxanthine phosphoribosyl transferase (HPRT) [10,6]. Clinical symptoms of LND are hyperuricemia, gouty arthritis, mental retardation, dystonia, spasticity, delayed motor development and a compulsive form of self-injurious behavior. The link between HPRT deficiency and the neuropsychiatric symptoms is unknown. To study the biochemical basis for the neuropsychiatric symptoms in LND, a HPRT knock-out mouse was generated [15]. Similar to LND patients, there are abnormalities in dopaminergic neurotransmission in the HPRT knock-out mouse [7,16]. In addition, several HPRT-deficient cell lines including primary human skin fibroblasts, immortalized mouse skin fibroblasts, mouse Neuro2a neuroblastoma cells and rat B103 neuroblastoma are used as biochemical models for LND [18,2,4,12,11]. In a recent study [11] we showed that nucleoside 5′-triphosphatase (NTPase) activity in B103- and Neuro2a cell membranes is reduced in HPRT-deficiency. In contrast, in mouse skin fibroblast membranes, NTPase activity is increased in HPRT deficiency. Thus, altered NTPase activity is a hallmark of HPRT deficiency and these changes are cell type- and species-specific. However, it is very difficult to reveal the molecular identity of the NTPase(s) in complex systems by measuring enzyme activity. Specifically, analysis of enzyme activity with various substrates and inhibitors revealed monophasic kinetics in control- and HPRT-deficient cells [11], suggesting that a single protein species accounts for the observed activity. However, small contributions of multiple protein species to the overall enzyme kinetics may be missed in such biochemical analysis. A likely candidate gene family responsible for the alterations in NTPase activity in HPRT-deficiency are the ecto-nucleoside 5′-triphosphate diphosphohydrolases (NTPDases) [17,13]. In fact,

*Abbreviations:* HPRT, hypoxanthine phosphoribosyl transferase; LND, Lesch-Nyhan disease; NTP, nucleoside 5′-triphosphate; NTPase, nucleoside 5′-triphosphatase; NTPDase, ecto-nucleoside 5′-triphosphate diphosphohydrolase; RT-PCR, reverse transcriptase polymerase chain reaction

* Corresponding author at: Department of Pharmacology and Toxicology, University of Regensburg, D-93040 Regensburg, Germany. Tel.: +49 941 943 4770; fax: +49 941 943 4772.
*E-mail address:* roland.seifert@chemie.uni-regensburg.de (R. Seifert).

0304-3940/$ – see front matter © 2007 Elsevier Ireland Ltd. All rights reserved.
doi:10.1016/j.neulet.2007.04.004

there is evidence that these enzymes play a role in neuronal development, which is disturbed in LND, and in the regulation of signal transduction mediated *via* purinergic receptors. It is also emerging that various NTPDase isoforms play distinct roles in neuronal development and signal transduction [17,13]. Therefore, we examined expression of NTPDases 1–6 in B103 cells, Neuro2a cells and skin fibroblasts by reverse transcriptase polymerase chain reaction (RT-PCR) and restriction enzyme digestion of amplified cDNA fragments.

Immortalized mouse skin fibroblasts from control mice and HPRT knock-out mice, rat B-103 control and HPRT-deficient B103 cells and mouse Neuro2a control and HPRT-deficient Neuro2a cells were cultured and passaged under the conditions described in [11]. HPRT-deficiency of cell clones used for experiments was confirmed with the 6-thioguanine resistance test [11]. Cell membranes were prepared as described [11].

RT-PCR analysis was performed similarly as the previously described protocol [14]. In brief, confluent cells from a 25 $cm^2$ culture were harvested with a cell scraper, and mRNA was isolated with the RNeasy kit from Qiagen (Hilden, Germany) and treated with RNase-free DNase. mRNA concentration was determined photometrically and reverse-transcribed using the First Strand cDNA synthesis kit from GE Healthcare (Munich, Germany) and oligo-dT as primer. cDNA was stored at −80 °C until PCR amplification. Primers were chosen in such a way that for each NTPDase, fragments of unique length were generated. Moreover, the primers were designed to include an internal diagnostic restriction enzyme site within the amplified sequence, producing unique fragment patterns for each NTPDase. Table 1 summarizes all relevant information regarding PCR analysis of NTPDases 1 and 3–6.

For amplification of NTPDase 1, Turbo-*Pfu* (Fermentas, St. Leon-Rot, Germany) was used. For amplification of other NTPDases, *Taq* isopolymerase (Qiagen) was used. Reaction mixtures contained 2 μg of cDNA, dNTPs (2.5 mM each), 2 μl *Pfu*- or *Taq* buffer (10×), 2 μl dimethyl sulfoxide, and forward primer and reverse primer. The total reaction volume was 20 μl. In preliminary experiments, annealing temperatures were optimized using the Biometra T-Gradient thermocycler (Biometra, Göttingen, Germany). For NTPDase 1, the optimal annealing temperature was 60 °C, for NTPDases 3 and 4 57 °C and for NTPDases 5 and 6 50 °C. Elongation was performed for 60 s (fragments <1 kbp) or 90 s (fragments >1 kbp) at 72 °C (35 cycles). Thereafter, a final extension for 10 min at 72 °C was performed. Following PCR amplification, 5 μl of loading buffer (5×) were added to samples, and bands were separated on gels containing 1.5% agarose (mass/vol) for 45 min at 100 V. Bands were visualized by ethidium bromide staining under UV light using the 100 bp and 1 kbp DNA standard ladders from New England Biolabs (Frankfurt/Main, Germany). Following visualization, bands were cut out from gels, and DNA was isolated using the QIAEX-II kit (Qiagen). Purified DNA was incubated for 2 h at 37 °C with the appropriate restriction enzymes (*Bsr*GI, *Acc*I, *Sac*I, *Hinc*II, New England Biolabs). Thereafter, digested DNA was separated on gels containing 2% (mass/vol) agarose and visualized by ethidium bromide staining under UV light.

Table 1
Overview on primers, National Center for Biotechnology GenBank accession numbers, expected PCR product length, internal restriction enzyme, position of restriction enzyme site in open reading frame and length of digested DNA fragments for NTPDases 1 and 3–6 from rat and mouse

| NTPDase | Forward primers (F) and reverse primers (R) | Genbank accession numbers | PCR product length (bp) | Internal restriction enzyme | Position of restriction enzyme site in open reading frame | Length of digested DNA fragments (bp, 5′ → 3′) |
|---|---|---|---|---|---|---|
| 1 (rat) | F: 5′-GAT CAT CAC TGG GCA GGA GGA AGG-3′<br>R: 5′-AAG ACA CCG TTG AAG GCA CAC TGG-3′ | U81295 | 542 | *Bsr*GI | 740/741 | 302, 239 |
| 1 (mouse) | F: 5′-GGC TGT GAT AGC TTT G-3′<br>R: 5′-AGC ATG GGT CCT TAA G-3′ | AF037366 | 763 | *Acc*I | 377/378 | 466, 296 |
| 3 (rat) | F: 5′-GCT ACT TCA AGT CCC A-3′<br>R: 5′-AAT CAG AAT CCA CTG C-3′ | NM_178106 | 1103 | *Sac*I | 1217/1218 | 732, 371 |
| 3 (mouse) | F: 5′-GCT ACT TCA AGT CCC A-3′<br>R: 5′-AAT CAG AAT CCA CTG C-3′ | AY714060 | 1103 | *Sac*I | 1217/1218 | 732, 371 |
| 4 (rat) | F: 5′-ATG GGG AGG ATT GGC A-3′<br>R: 5′-CTT CCT CCA TCC ACA G-3′ | XM_34134 | 1783 | *Hinc*II | 750/751 | 750, 1033 |
| 4 (mouse) | F: 5′-ATG GGG AGG ATT GGC A-3′<br>R: 5′-CTT CCT CCA TCC ACA G-3′ | NM_026174 | 1807 | *Hinc*II | 750/751 | 750, 1057 |
| 5 (rat) | F: 5′-TCT TGT CTT CCA TGT G-3′<br>R: 5′-GTT CAC TTT CTT TGT G-3′ | NM199394 | 1117 | *Sac*I | 768/769 | 446, 671 |
| 5 (mouse) | F: 5′-TCT TGT CTT CCA TGT G-3′<br>R: 5′-GTT CAC TTT CTT TGT G-3′ | NMU238636 | 1117 | *Sac*I | 768/769 | 446, 671 |
| 6 (rat) | F: 5′-GTT CAT CTA TGT TGC C-3′<br>R: 5′-GGG AGT CGA TGT AAT G-3′ | AJ277748 | 1264 | *Hinc*II | 612/613 | 538, 726 |
| 6 (mouse) | F: 5′-GTT CAT CTA TGT TGC C-3′<br>R: 5′-GGG AGT CGA TGT AAT G-3′ | NM_172117 | 1264 | *Hinc*II | 612/613 | 538, 726 |

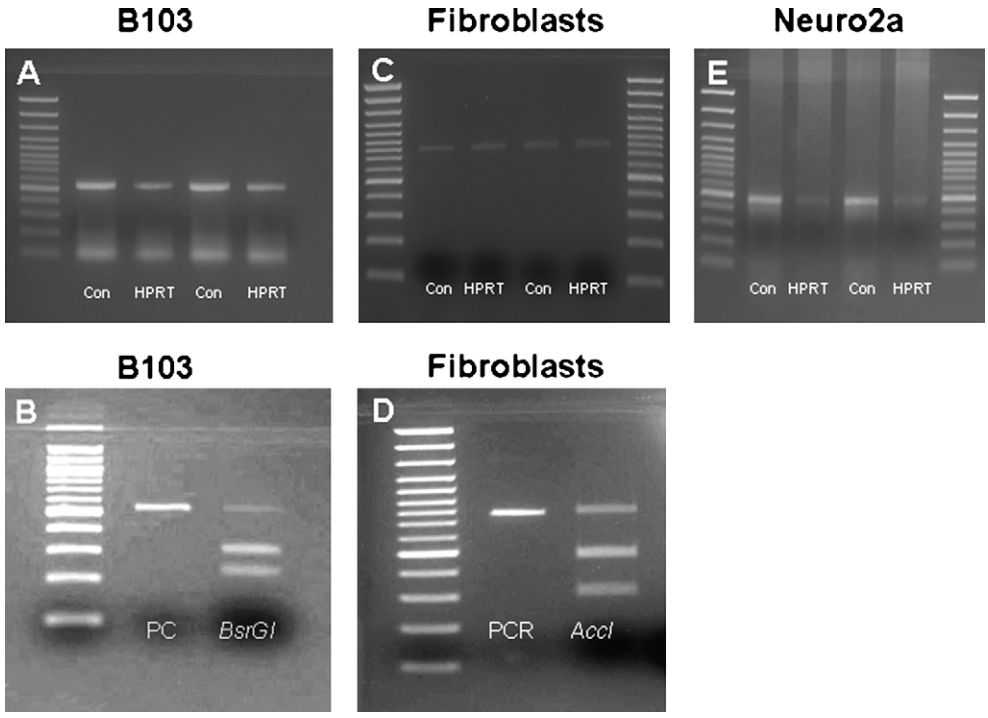


Fig. 1. Expression of NTPDase 1. Reverse-transcribed mRNA from B103 cells (A), fibroblasts (C) and Neuro2a cells (E) was amplified by PCR using appropriate primer pairs. Amplified cDNA was separated on agarose gels calibrated with 100 bp standard. The bold band represents the 500 bp band. Con, control cells; HPRT, HPRT-deficient cells. For each cell type, PCRs from two independent cDNA preparations are shown. (B) Undigested PCR product (PCR) and *Bsr*GI-digested PCR product (*Bsr*GI) from B103 control cells. (D) Undigested PCR product (PCR) and *Acc*I-digested PCR product (*Acc*I) from fibroblasts. The 100 bp standard was used in panels B and D.

Membranes were prepared as described [11]. SDS-PAGE and immunoblotting were performed as described [5]. Proteins were transferred onto nitrocellulose membranes and probed with NTPDase 1 antibody C92B2 [3] or NTPDase 2 antibody BZ3B4F [1]. Immunoreactive proteins were visualized using the enhanced chemiluminescence system (GE Healthcare). As positive control, we used Chinese hamster ovary (CHO) cell membranes (2 μg of pro-

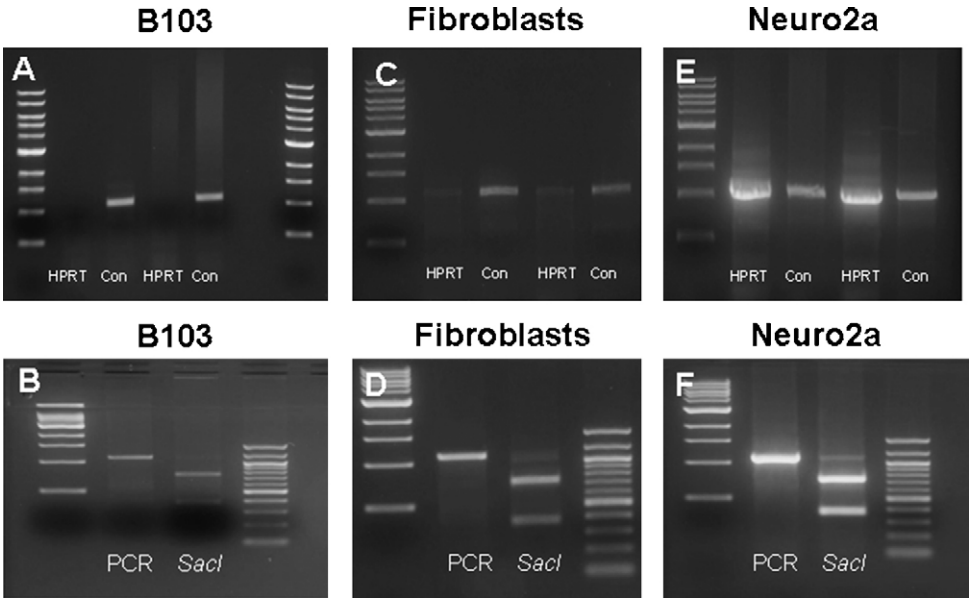


Fig. 2. Expression of NTPDase 3. Reverse-transcribed mRNA from B103 cells (A), fibroblasts (C) and Neuro2a cells (E) was amplified by PCR using appropriate primer pairs. Amplified cDNA was separated on agarose gels calibrated with 1 kbp standard. The bold band represents the 3 kbp band. Con, control cells; HPRT, HPRT-deficient cells. For each cell type, PCRs from two independent cDNA preparations are shown. (B) Undigested PCR product (PCR) and *Sac*I-digested PCR product (*Sac*I) from B103 control cells. (D) Undigested PCR product (PCR) and *Sac*I-digested PCR product (*Sac*I) from fibroblasts. (F) Undigested PCR product (PCR) and *Sac*I-digested PCR product (*Sac*I) from Neuro2a cells. In panels B, D and F, the 1 kbp standard was used on the left side, and the 100 bp standard was used on the right side.

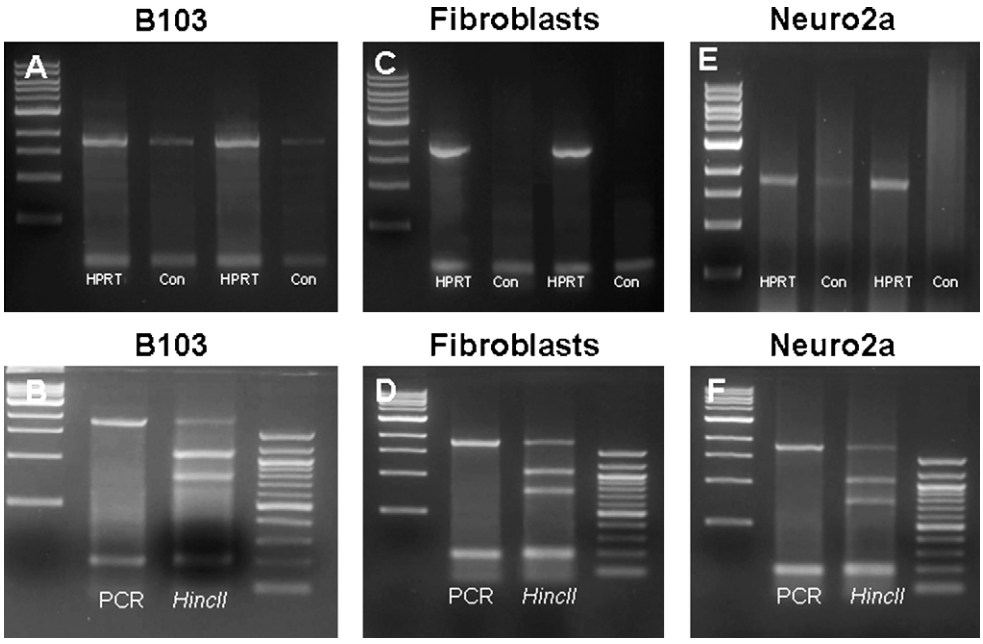


Fig. 3. Expression of NTPDase 4. Reverse-transcribed mRNA from B103 cells (A), fibroblasts (C) and Neuro2a cells (E) was amplified by PCR using appropriate primer pairs. Amplified cDNA was separated on agarose gels calibrated with 1 kbp standard. The bold band represents the 3 kbp band. Con, control cells; HPRT, HPRT-deficient cells. For each cell type, PCRs from two independent cDNA preparations are shown. (B) Undigested PCR product (PCR) and *Hinc*II-digested PCR product (*Hinc*II) from B103 control cells. (D) Undigested PCR product (PCR) and *Hinc*II-digested PCR product (*Hinc*II) from fibroblasts. (F) Undigested PCR product (PCR) and *Hinc*II-digested PCR product (*Hinc*II) from Neuro2a cells. In panels B, D and F, the 1 kbp standard was used on the left side, and the 100 bp standard was used on the right side.

tein per lane) overexpressing either NTPDase 1 or NTPDase 2.

The data shown in Figs. 1–5 were reproduced at least three times with one given mRNA preparation. Figs. 1–5 (panels A, C and E) show representative PCR results obtained for two independent cDNA preparations.

B103 control cells expressed higher levels of NTPDase 1 (542 bp band) than HPRT-deficient B103 cells (Fig. 1A). In fibroblasts, NTPDase 1 expression (763 bp band) was relatively low, and differences between control and HPRT-deficient cells were not clear (Fig. 1C). Restriction enzyme analysis confirmed that the correct bands were amplified (302 and 239 bp for rat

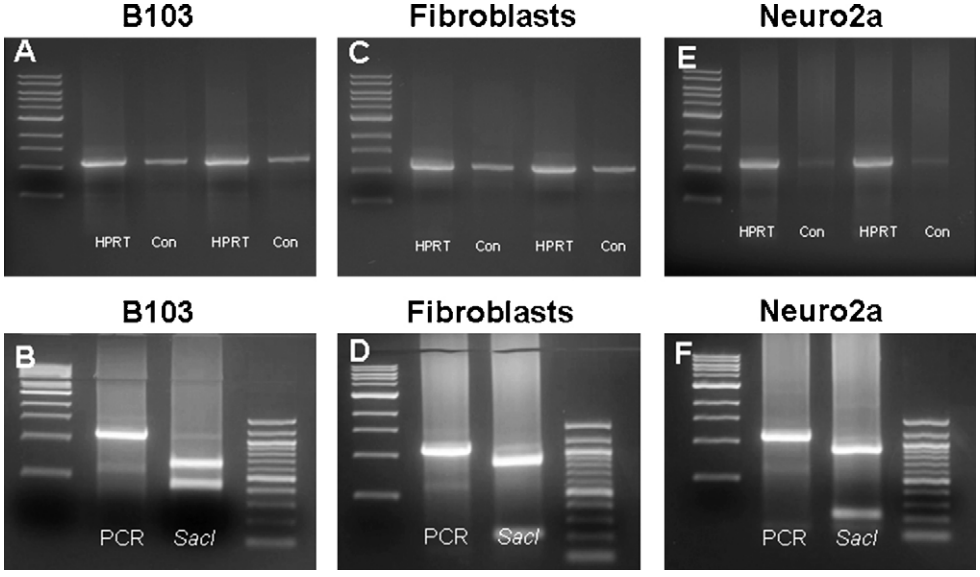


Fig. 4. Expression of NTPDase 5. Reverse-transcribed mRNA from B103 cells (A), fibroblasts (C) and Neuro2a cells (E) was amplified by PCR using appropriate primer pairs. Amplified cDNA was separated on agarose gels calibrated with 1 kbp standard. The bold band represents the 3 kbp band. Con, control cells; HPRT, HPRT-deficient cells. For each cell type, PCRs from two independent cDNA preparations are shown. (B) Undigested PCR product (PCR) and *Sac*I-digested PCR product (*Sac*I) from B103 control cells. (D) Undigested PCR product (PCR) and *Sac*I-digested PCR product (*Sac*I) from fibroblasts. (F) Undigested PCR product (PCR) and *Sac*I-digested PCR product (*Sac*I) from Neuro2a cells. In panels B, D and F, the 1 kbp standard was used on the left side, and the 100 bp standard was used on the right side.

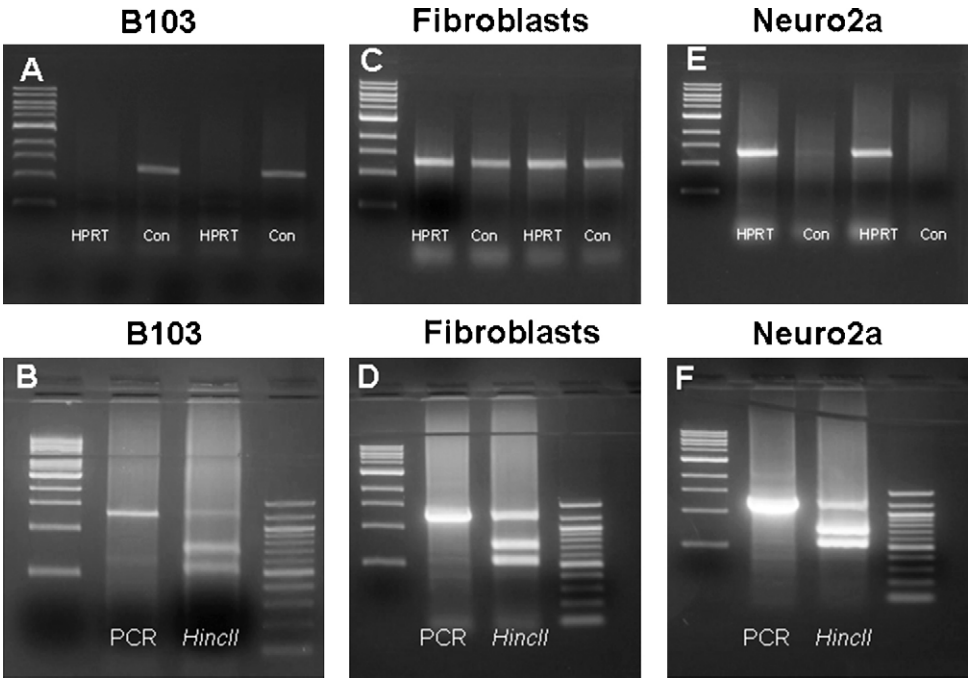


Fig. 5. Expression of NTPDase 6. Reverse-transcribed mRNA from B103 cells (A), fibroblasts (C) and Neuro2a cells (E) was amplified by PCR using appropriate primer pairs. Amplified cDNA was separated on agarose gels calibrated with 1 kbp standard. The bold band represents the 3 kbp band. Con, control cells; HPRT, HPRT-deficient cells. For each cell type, PCRs from two independent cDNA preparations are shown. (B) Undigested PCR product (PCR) and *Hinc*II-digested PCR product (*Hinc*II) from B103 control cells. (D) Undigested PCR product (PCR) and *Hinc*II-digested PCR product (*Hinc*II) from fibroblasts. (F) Undigested PCR product (PCR) and *Hinc*II-digested PCR product (*Hinc*II) from Neuro2a cells. In panels B, D and F, the 1 kbp standard was used on the left side, and the 100 bp standard was used on the right side.

B103 cells (Fig. 1B) and 466 and 296 bp for mouse fibroblasts (Fig. 1D). The digest for both PCR products was not complete, explaining the third band corresponding to the initial PCR product. In Neuro2a cells, we also expected to amplify a 763 bp fragment, but this was not seen (Fig. 1E), even after assessing multiple reaction conditions including different annealing temperatures, different polymerases and template/primer ratios. Given the positive results with the other cell lines using the same primers and PCR reaction conditions, these data probably reflect the absence of NTPDase 1 in Neuro2a cells.

We also performed immunoblotting studies with the NTPDase 1 antibody C92B2. In NTPDase 1-expressing CHO cells, we observed the expected bands (data not shown) [17,13]. However, no specific bands were detected in B103-, Neuro2a- and fibroblast cell membranes (data not shown).

We undertook numerous efforts (various primer pairs, two different polymerases, different annealing temperatures and different template/primer ratios) to detect expression of NTPDase 2 in the various cell types. However, all PCR efforts were unsuccessful and no specific bands could be amplified. We also performed immunoblotting studies with the NTPDase 2 antibody BZ3B4F. While in NTPDase 2-expressing CHO cells, the expected band was detected (data not shown) [17,13], no specific bands were detected in B103-, Neuro2a- and fibroblast cell membranes (data not shown).

In B103 control cells, strong expression of NTPDase 3 was seen (1103 bp), whereas the enzyme was absent in HPRT deficiency (Fig. 2A). In control fibroblasts, we detected a much stronger NTPDase 3 signal than in HPRT deficiency (Fig. 2C). In contrast, in Neuro2a cells, HPRT deficiency was associated with increased NTPDase 3 expression (Fig. 2E). Restriction enzyme analysis confirmed that the correct bands (732 and 371 bp) were amplified (Fig. 2B, D and F).

Unlike with NTPDases 1 and 3 (Figs. 1 and 2), the expression pattern of NTPDase 4 was consistent in all three cell lines studied. Specifically, expression of NTPDase 4 (1807 bp band in rat B103 cells and 1783 bp band in mouse fibroblasts and mouse Neuro2a cells) was much higher in HPRT-deficient cell lines than in control cell lines (Fig. 3A, C and E). Restriction enzyme analysis confirmed that the correct bands were amplified (750 bp and 1033 bp fragments for B103 cells and 750 bp and 1057 bp fragments for fibroblasts and Neuro2a cells) (Fig. 3B, D and F). Again, we observed incomplete digestion of PCR fragments.

Similar to the data obtained for NTPDase 4, HPRT deficiency was associated with increased expression of NTPDase 5 (1117 bp band) relative to control in all three cell lines (Fig. 5A, C and E). The difference in expression was more pronounced for Neuro2a cells than for B103 cells and fibroblasts. Restriction enzyme analysis confirmed that the correct bands (671 and 446 bp) were amplified (Fig. 5B, D and F).

A heterogeneous picture emerged with respect to NTPDase 6 expression. In particular, in B103 cells, HPRT deficiency was associated with a loss of NTPDase 6 expression (1264 bp band) (Fig. 5A), whereas in Neuro2a cells, NTPDase 6 was only observed in HPRT deficiency (Fig. 5C). In fibroblasts, NTPDase 6 expression was slightly higher in HPRT-deficient cells than in control cells (Fig. 5B). Restriction enzyme analysis confirmed

that the correct bands (538 and 726 bp) were amplified (Fig. 5B, D and F).

Our previous study on the enzymatic analysis of NTPase activity indicated that HPRT deficiency is associated with changes in enzyme activity (increase or decrease) and that the changes in activity are dependent on the species and the cell type studied [11]. Our RT-PCR studies yielded very complex results. Specifically, in rat B103 cells, HPRT deficiency is associated with strongly decreased expression of NTPDases 3 and 6 and weakly decreased expression of NTPDase 1, but the expression of NTPDases 4 and 5 is actually increased. Even more strikingly, in mouse Neuro2a cells, only increases in NTPDase expression were observed. In mouse fibroblasts, NTPDase 3 expression decreased, whereas NTPDase 4–6 expression actually increased. Thus, our present expression data for individual NTPDase isoenzymes confirm the notion that secondary biochemical changes in HPRT-deficiency are cell type- and species-specific [12,11].

As an explanation for the discrepancies between the NTPase activity reductions in HPRT deficiency for B103- and Neuro2a cells and the increase in NTPase activity in HPRT deficiency for mouse fibroblasts on one hand and the complex changes in NTPDase expression on the other hand, it is possible that not all of the PCR-amplified cDNAs are actually translated into functionally active NTPDase proteins in intact cells. In fact, dissociations between mRNA- and protein expression are commonly observed in neuronal cells [8,9]. Additionally, the specific activities of various NTPDases may differ from each other. Moreover, NTPDases differ from each other in their substrate-specificity [13]. Unfortunately, the limited sensitivity of the NTPDase 1 and 2 antibodies and the non-availability of antibodies for NTPDases 3–6 did not allow us to further study NTPDase expression at the protein level.

Regardless of which precise enzyme actually accounts for the substantial differences in NTPase activity as a consequence of HPRT deficiency [11], our present expression study on a focused set of candidate target genes clearly shows that NTPDase isoenzyme expression is highly complex. Our findings point to distinct functional roles of individual NTPDase isoforms. These complex changes in NTPDase expression may reflect (insufficient) attempts of cells to compensate for the primary alteration of nucleotide metabolism in HPRT deficiency. Depending on the overall changes in NTPDase isoenzyme expression and the specific activities of isoenzymes, the net result may be an increase or a decrease in NTPDase activity.

Finally, it should be emphasized that our present study was performed with rat and mouse cell lines. Given the well-known species-specificity of biochemical changes in HPRT-deficiency [18,2,4,12,11], one has to be cautious with extrapolations to LND. Accordingly, in future studies, human neuronal cell culture cell lines will have to be studied.

## Acknowledgements

We thank Gertraud Wilberg for expert help with the cell culture, Corinna Matzdorf for technical advice on RT-PCR, David Schnell for advice on primer design and Dr. Herbert Zimmermann (Johann-Wolfgang Goethe-Universität, Frankfurt/Main, Germany) for support with the immunoblotting studies and helpful discussions. This project was supported by a grant of the Lesch-Nyhan Syndrome Children's Research Foundation to R.S.

## References

[1] N. Braun, J. Sevigny, S.K. Mishra, S.C. Robson, S.W. Barth, R. Gerstberger, K. Hammer, H. Zimmermann, Expression of the ecto-ATPase2 in the germinal zones of the developing and adult brain, Eur. J. Neurosci. 17 (2003) 1355–1364.

[2] G.P. Connolly, J.A. Duley, N.C. Stacey, Abnormal development of hypoxanthine-guanine phosphoribosyltransferase-deficient CNS neuroblastoma, Brain Res. 918 (2001) 20–27.

[3] K. Enjyoji, J. Sevigny, Y. Lin, P.S. Frenette, P.D. Christie, J.S. Esch 2nd, M. Imai, J.M. Edelberg, H. Rayburn, M. Lech, D.L. Beeler, E. Csizmadia, D.D. Wagner, S.C. Robson, R.D. Rosenberg, Targeted disruption of cd39/ATP diphosphohydrolase results in disordered hemostasis and thromboregulation, Nat. Med. 5 (1999) 987–988.

[4] L.D. Fairbanks, G. Jacomelli, V. Micheli, T. Slade, H.A. Simmonds, Severe pyridine nucleotide depletion in fibroblasts from Lesch-Nyhan patients, Biochem. J. 366 (2002) 265–272.

[5] P. Heine, N. Braun, A. Heilbronn, H. Zimmermann, Functional characterization of rat ecto-ATPase and ecto-ATP-diphosphohydrolase after heterologous expression in CHO cells, Eur. J. Biochem. 262 (1999) 102–109.

[6] H.A. Jinnah, T. Friedmann, Lesch-Nyhan disease and its variants, in: C. Scriver, A. Beaudet, W. Sly, D. Valle, K.W. Kinzler, B. Vogelstein (Eds.), The Metabolic Basis of Inherited Disease, eighth ed., McGraw-Hill, New York, 2000, Chapter 107.

[7] H.A. Jinnah, B.E. Wojcik, M. Hunt, N. Narang, K.Y. Lee, M. Goldstein, J.K. Wamsley, P.J. Langlais, T. Friedmann, Dopamine deficiency in a genetic mouse model of Lesch-Nyhan disease, J. Neurosci. 14 (1994) 1164–1175.

[8] E.J. Mufson, S.E. Counts, S. Che, S.D. Ginsberg, Neuronal gene expression profiling: uncovering the molecular biology of neurodegenerative disease, Prog. Brain Res. 158 (2006) 197–222.

[9] S.B. Nelson, C. Hempel, K. Sugino, Probing the transcriptome of neuronal cell types, Curr. Opin. Neurobiol. 16 (2006) 571–576.

[10] W.L. Nyhan, The recognition of Lesch-Nyhan syndrome as an inborn error of purine metabolism, J. Inherit Metab. Dis. 20 (1997) 171–178.

[11] C.S. Pinto, H.A. Jinnah, T.L. Shirley, W.L. Nyhan, R. Seifert, Altered membrane NTPase activity in Lesch-Nyhan disease fibroblasts: comparison with HPRT knock-out mice and HPRT-deficient cell lines, J. Neurochem. 93 (2005) 1579–1586.

[12] C.S. Pinto, R. Seifert, Decreased GTP-stimulated adenylyl cyclase activity in HPRT-deficient human and mouse fibroblast and rat B103 neuroblastoma cell membranes, J. Neurochem. 96 (2006) 454–459.

[13] S.C. Robson, J. Sévigny, H. Zimmermann, The E-NTPDase family of ectonucleotidases: structure function relationships and pathophysiological relevance, Purinergic Signal. 2 (2006) 409–430.

[14] K. Wenzel-Seifert, R. Seifert, Molecular analysis of $\beta_2$-adrenoceptor coupling to $G_s$-, $G_i$-, and $G_q$-proteins, Mol. Pharmacol. 58 (2000) 954–966.

[15] D.J. Williamson, M.L. Hooper, D.W. Melton, Mouse models of hypoxanthine phosphoribosyltransferase deficiency, J. Inherit Metab. Dis. 15 (1992) 665–673.

[16] D.F. Wong, J.C. Harris, S. Naidu, F. Yokoi, S. Marenco, R.F. Dannals, H.T. Ravert, M. Yaster, A. Evans, O. Rousset, R.N. Bryan, A. Gjedde, M.J. Kuhar, G.R. Breese, Dopamine transporters are markedly reduced in Lesch-Nyhan disease in vivo, Proc. Natl. Acad. Sci. U.S.A. 93 (1996) 5539–5543.

[17] R. Zimmermann, Extracellular metabolism of ATP and other nucleotides, Naunyn Schmiedebergs Arch. Pharmacol. 362 (2002) 299–309.

[18] E. Zoref-Shani, Y. Bromberg, S. Brosh, Y. Sidi, O. Sperling, Characterization of the alterations in purine nucleotide metabolism in hypoxanthine-guanine phosphoribosyltransferase-deficient rat neuroma cell line, J. Neurochem. 61 (1993) 457–463.